J. Fluid Mech. (1978), *vol.* 86, *part* 1, *pp.* 161–177
Printed in Great Britain

Symmetrical flow past a double wedge at high subsonic Mach numbers

By JEAN-JACQUES CHATTOT
Office Nationale d'Etudes et de Recherches Aérospatiales, 92320 Chatillon, France

(Received 20 October 1975 and in revised form 15 October 1977)

Symmetrical flow past a double wedge is studied for a high subsonic Mach number. The main features of the flow field are discussed in the physical and the hodograph plane. It is shown how a regular solution to the hodograph equation exhibits limit lines in the physical plane, which are eliminated through a 'cut' corresponding to the shock wave. In the case of the wedge it is assumed that the shock which is likely to be the most stable is the weakest possible.

The boundary-value problem is solved in the hodograph plane using Telenin's method, which has proved to be successful when dealing with equations of mixed type. The bounded analytic solution which is thus constructed is regular in the hodograph plane but presents three folds in the physical plane.

The computation is carried out for flow past a 4·5° half-angle wedge at a Mach number $M_\infty = 0{\cdot}89$. These figures are chosen so that the problem may be justifiably treated by potential theory, the entropy gradient behind the shock being negligible. In this case the mapping of the solution into the physical plane gives the pressure distribution along the double wedge, the sonic line and the shock wave. Of particular interest is the point where the sonic line meets the shock. This configuration is in agreement with the hypothesis of Nocilla, according to which the shock terminates in the supersonic domain. Experimental evidence cannot be obtained, however, because of the lack of resolution in this region.

1. Introduction

The fact that most jet aeroplanes now fly in the transonic range (and that possible future aeroplanes will be restricted to it) explains why there has been such a large amount of work done in this area of fluid mechanics over the past decade. But interest in this topic dates back to earlier in the century, when mathematicians as well as fluid dynamicists found themselves confronted with a new type of equation giving rise to a new type of boundary-value problem. The mixed-type equation governing transonic flows has been solved to describe desirable shock-free flows past certain types of smooth aerofoils for certain values of the Mach number and incidence. The validity of these theoretical solutions has now been confirmed experimentally; formerly the existence of supercritical shock-free flows was in doubt. Usually a large embedded supersonic region is terminated by a shock.

At subsonic free-stream Mach numbers, the flow past a double wedge exhibits a stable recompression shock which terminates the bounded supersonic region. In this work a method is set up for solving such a flow, taking the shock into account, with

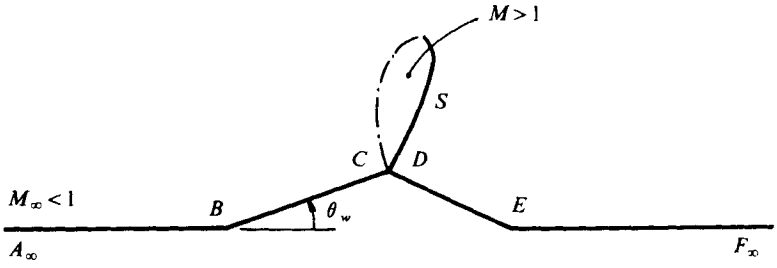

FIGURE 1. Transonic flow past a symmetrical double wedge.

the assumption that it terminates at the convex corner. The flow field is discussed in the physical as well as the hodograph plane. A boundary-value problem is posed in the hodograph plane, which will lead to a many sheeted physical plane. A shock is fitted in the flow field to eliminate the ill-behaved part of the physical plane. The problem is solved in the hodograph plane using Telenin's method and the transfer back to the physical plane is the subject of the last section.

2. Flow field in the physical plane

Telenin's method (Gilinskii, Telenin & Tinyakov 1964) is a numerical technique applicable to elliptic or mixed-type problems in which finite-difference calculations in selected co-ordinate directions are eliminated. It was originally developed to solve the supersonic blunt-body problem. In the present work it is applied to a somewhat different mixed-type problem, that of supercritical flow past a wedge. In this case the flow is subsonic everywhere except in a local embedded supersonic region above the mid-chord section. The outer boundary of this region consists of a sonic line which runs into a shock wave at the downstream end.

As shown in figure 1, in the physical plane we expect to have an analytic solution for the stream function $\psi(x, y)$ as a function of the physical co-ordinates (x, y) except along the curve S, where the derivatives are expected to have discontinuities. The curve S acts as a cut in this plane. The points B and E are singular points since the streamline $\psi = 0$ has a discontinuity in slope there, but these are stagnation points and we know the local solutions in the physical as well as the hodograph plane, because they are determined by incompressible theory. The point D, the foot of the shock in the physical plane, may be a point of discontinuity in the first or higher derivatives for the streamline $\psi = 0$. In the case of the wedge, the shock must run through the shoulder to eliminate possible limit lines. Since the physical plane is cut along the curve S this singularity presents no difficulties, provided that the characteristic through D does not reach the sonic line.

Working in the physical plane would require the solution of a nonlinear second-order partial differential equation for $\psi(x, y)$, which, with the increase in capacity of computing machines, is no longer an obstacle. Nevertheless, this solution would require an iteration process and therefore would be more time consuming. Also, the boundary condition at 'infinity' would not be as easy to apply as it is in the hodograph plane, since in any numerical computation we have to decide on which large rectangle we can reasonably apply this condition.

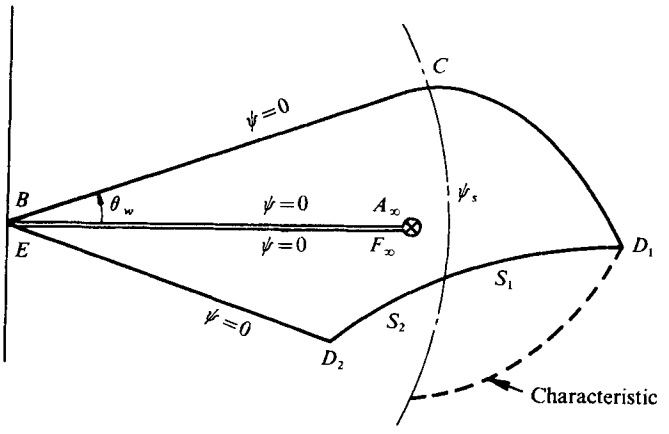

FIGURE 2. Hodograph for symmetrical flow past a double wedge.

3. Flow field in the hodograph plane (q, θ)

3.1. *Qualitative description of the flow*

The major reason for solving the flow past a double wedge is that the boundary of the mixed domain is known almost completely in the hodograph plane, which is usually not the case when one deals with an aerofoil of general shape. With the same notation as is adopted in the physical plane, the flow field is sketched in figure 2.

The streamline $\psi = 0$ is made up of the following segments: $A_\infty B$, which is part of the $\theta = 0$ axis; BE, which is a radial line at an angle θ_w to the axis $\theta = 0$; CD, which is an arc of a characteristic since we have locally a Prandtl–Meyer expansion; DE, which is also a radial line with polar angle $-\theta_w$; finally, EF_∞, on which $\theta = 0$. We do not know *a priori* the two images D_1 and D_2 of the point D in the hodograph, nor do we known the images S_1 and S_2 of the shock curve which correspond to the cut S in the physical plane. Now we are dealing with a bounded region and the point at infinity in the physical plane is mapped at a finite distance (A_∞, F_∞).

3.2. *Equation for the stream function*

The derivation of the Chaplygin equation for $\psi(q, \theta)$ can be found in any standard textbook dealing with the hodograph method. The derivation is based on the assumption that entropy variations are negligible throughout the flow field. This is valid for the transonic flows under consideration, since the local Mach number is everywhere close to unity and any shocks generated are weak. Chaplygin's equation is

$$\frac{(1-q^2)}{1-[(\gamma+1)/(\gamma-1)]q^2}q^2\frac{\partial^2\psi}{\partial q^2}+\frac{1+[(3-\gamma)/(\gamma-1)]q^2}{1-[(\gamma+1)/(\gamma-1)]q^2}q\frac{\partial\psi}{\partial q}+\frac{\partial^2\psi}{\partial\theta^2}=0, \tag{3.1}$$

where q is the flow speed non-dimensionalized by $\bar{q}_{\max} = [(\gamma+1)/(\gamma-1)]^{\frac{1}{2}}a^*$, a^* is the critical speed of sound and $\gamma = C_p/C_v$ is the specific-heat ratio. The transformation from the hodograph to the physical plane is realized through the following equations:

$$\frac{\partial x}{\partial q}=-\frac{1}{\rho q}\left[\frac{\cos\theta}{q}\left(1-\frac{q^2}{a^2}\right)\frac{\partial\psi}{\partial\theta}+\sin\theta\frac{\partial\psi}{\partial q}\right], \tag{3.2}$$

$$\frac{\partial x}{\partial \theta} = \frac{1}{\rho q}\left[\cos\theta q \frac{\partial \psi}{\partial q} - \sin\theta \frac{\partial \psi}{\partial \theta}\right], \tag{3.3}$$

$$\frac{\partial y}{\partial q} = \frac{1}{\rho q}\left[-\frac{\sin\theta}{q}\left(1-\frac{q^2}{a^2}\right)\frac{\partial \psi}{\partial \theta} + \cos\theta \frac{\partial \psi}{\partial q}\right], \tag{3.4}$$

$$\frac{\partial y}{\partial \theta} = \frac{1}{\rho q}\left[\sin\theta q \frac{\partial \psi}{\partial q} + \cos\theta \frac{\partial \psi}{\partial \theta}\right], \tag{3.5}$$

where $$\rho = (1-q^2)^{(1/\gamma-1)}, \quad \rho \text{ being non-dimensionalized by } \bar{\rho}_{\text{stag}}. \tag{3.6}$$

4. Boundary-value problem in the hodograph plane

The function $\psi(q,\theta)$ has to satisfy $\psi = 0$ on the open boundary $A_\infty BCD_1 + D_2EF_\infty$; also $\psi(q,\theta)$ has to satisfy a homogeneous first-order equation on S of the form

$$F[\partial\psi/\partial q, \partial\psi/\partial\theta, q_1, \theta_1, q_2, \theta_2, dq/d\theta] = 0,$$

where (q_1,θ_1) and (q_2,θ_2) are two points on S corresponding to the same streamline (i.e. $\psi(q_1,\theta_1) = \psi(q_2,\theta_2)$), $dq/d\theta$ being the slope of S at either point 1 or point 2. We shall be more explicit later.

We need to have a singular point inside the domain, otherwise $\psi(q,\theta) = 0$ would satisfy all the boundary conditions. Indeed, the image of the point at infinity in the physical plane is a singular point for the hodograph equations. It is a branch point for ψ and the line $A_\infty B$ (or $F_\infty E$) is a common line for the two Riemann surfaces corresponding to the upper and lower halves of the physical plane (i.e. $y \geqslant 0$ or $y \leqslant 0$). In the neighbourhood of A_∞ the potential $\psi(q,\theta)$ has a leading term as given by Germain (1962):

$$\left.\begin{aligned} \psi_s(q,\theta) &= Kr^{-\frac{1}{2}}\sin\tfrac{1}{2}\omega, \\ \sin\omega = \theta/r, \quad r^2 &= \theta^2 + \delta(\gamma)(q-q_\infty)^2, \end{aligned}\right\} \tag{4.1}$$

where K is a constant multiplier (corresponding to a change in scale in the physical plane). Here we exclude this singular point by enclosing it by a 'small circle' and a cut running from E to F_∞ and A_∞ to B.

Clearly there are some other singular points: the two stagnation points B and E. But as pointed out in § 2, we know the local incompressible solution and we can match it to the compressible one so that we get a continuous description of the flow field.

Point C is also a singular point for ψ since the analytic expression for the streamline $\psi = 0$ changes there. From a straight line it changes to an epicycloid. There is a discontinuity in the second and higher derivatives. Here we suppress this weak singularity by replacing the exact boundary by an analytical curve as close as necessary to the combination of a straight line and an epicycloid. This, of course, implies that we are no longer solving for the exact wedge, but for a body which is bounded by an analytical curve with a very small radius of curvature at C; the solution is expected to be altered only in a very small neighbourhood of C.

If the characteristic issuing from D_1 does not meet the sonic line inside the domain (dashed line on figure 2), then the supersonic fluid particles moving around the wedge shoulder reach the cut S without warning, so that neither D_1 nor D_2 is a singular point. This is the criterion mentioned in § 2. But the difficulty of solving in a domain the

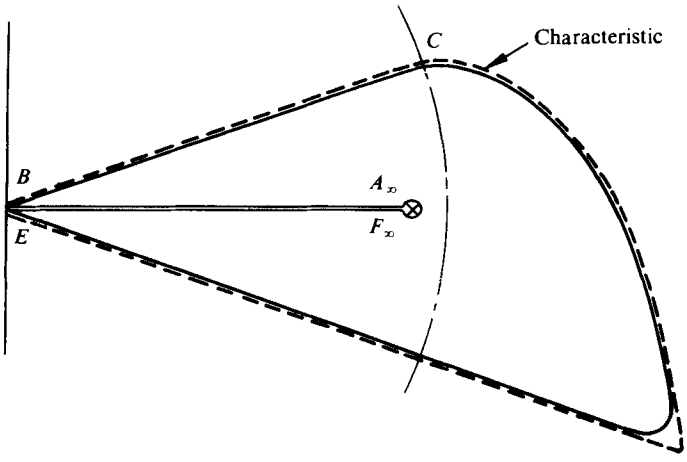

FIGURE 3. Boundary of the hodograph for the computation.

boundary of which is not completely known in advance remains. To overcome this a solution for $\psi(\eta, \theta)$ is first found within a different domain in which the existence of the shock curve is ignored. Once this flow field has been determined, the shock can be fitted inside it to satisfy all requirements.

If there were no shock the domain, in the hodograph plane, would be as shown on figure 3 (dashed boundary). We then solve for the domain inside the solid curve (which is an analytical approximation to the exact boundary) in the class of C^∞ solutions.

5. The multi-sheeted physical plane: necessity for a shock

Once the boundary-value problem (§ 4) has been solved by means of a numerical method, it is clear that in the hodograph plane certain streamlines are going to be tangential to characteristics in the supersonic subdomain, at least twice. This is a consequence of the shape of the boundary and the analyticity of the solution (figure 4). Eventually, for a high enough value of the stream function, there is no such point of contact. The last streamline which is tangential to a characteristic has the geometric property of having the same curvature as the characteristic at the point of contact (double point). By joining these points together we obtain two limit lines L_1 and L_2, which merge together at the double point.

On these two lines the Jacobian of the transformation from the hodograph to the physical plane vanishes: $J = \partial(x, y)/\partial(q, \theta) = 0$, as demonstrated by Lighthill (1953). He demonstrated also that to a regular point on the limit line there corresponds, in the physical plane, a point where one characteristic is tangential (this gives in the physical plane a geometric interpretation to the limit line, as an envelope of one family of characteristics) and the other forms a cusp together with the streamline. However, since some streamlines are entirely subsonic, the limit line in the physical plane will have a cusp which corresponds to the double point in the hodograph. The streamline passes directly through this point in the physical plane. The physical plane is three-sheeted as shown on figure 5.

The limit lines are a mathematical obstacle to isentropic flow taking place under the

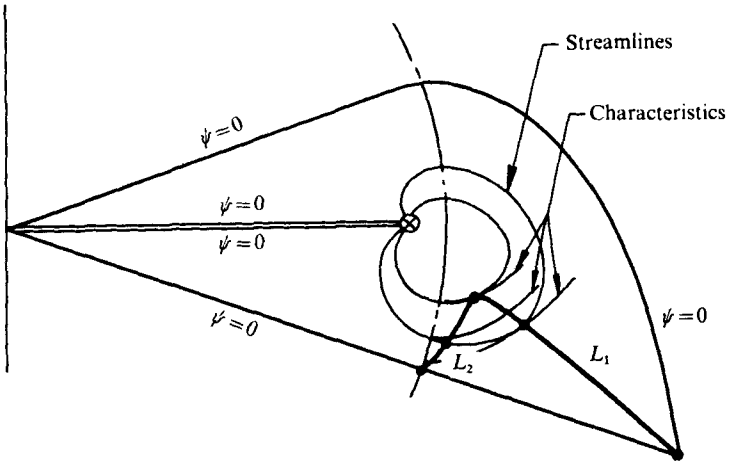

FIGURE 4. Limit lines in the hodograph.

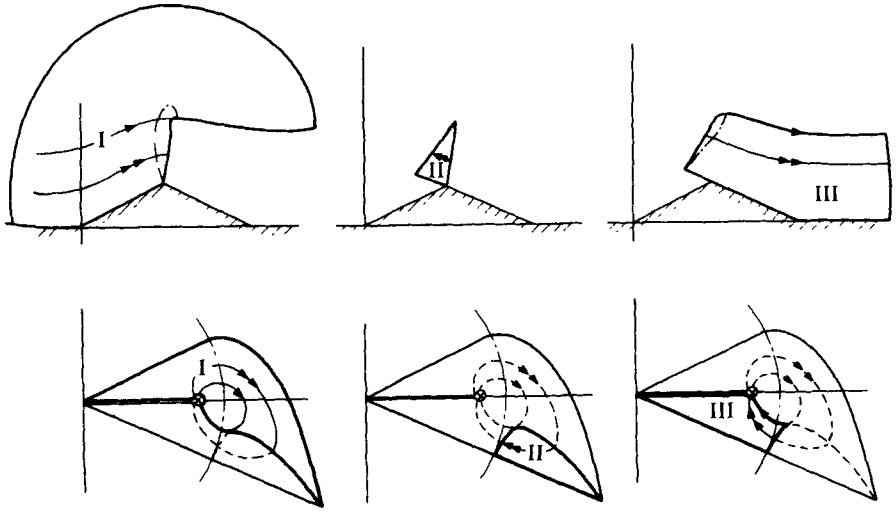

FIGURE 5. The multi-sheeted physical plane and the corresponding hodograph.

present boundary conditions. To recover a physically meaningful flow field in the physical plane we must fit a shock which will remove the ill-behaved part of the flow and leave a domain of the type shown on figures 1 and 2.

The shock must satisfy the following conditions.

(i) Continuity of the stream function across it, so that if we denote by (q_1, θ_1) and (q_2, θ_2) the images in the hodograph plane of a point (y_s, x_s) on the shock curve in the physical plane (see figure 6) we have

$$\psi(q_1, \theta_1) = \psi(q_2, \theta_2). \tag{5.1}$$

(ii) Shock relations, which are easily derived in hodograph co-ordinates:

$$\cos^2(\theta_1 - \theta_2) - \frac{\gamma+1}{2\gamma}\frac{q_1^2+q_2^2+2(\gamma-1)/(\gamma+1)}{q_1 q_2}\cos(\theta_1-\theta_2) + \frac{1}{\gamma} + \frac{\gamma-1}{2\gamma}\frac{q_1^2+q_2^2}{q_1^2 q_2^2} = 0. \tag{5.2}$$

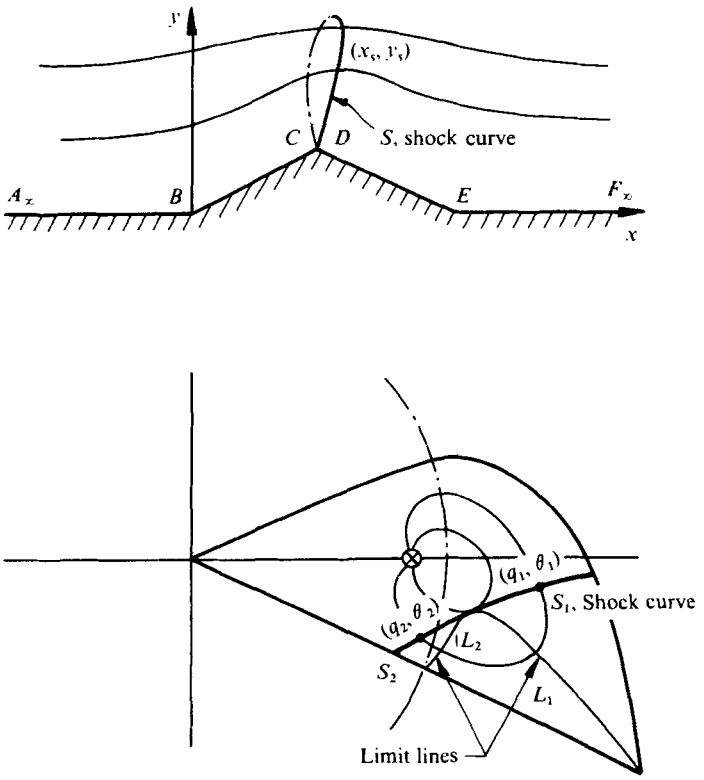

FIGURE 6. The shock wave in the physical plane and the hodograph plane.

(iii) A differential equation along the upstream or downstream part of the shock, stating that they map onto the same curve in the physical plane. Taking into account (3.2)–(3.5) gives

$$\left(\frac{\partial\psi}{\partial q}\right)_2 \left\{q_1 \sin(\theta_1-\theta_2) + [-q_2 + q_1\cos(\theta_1-\theta_2)]\, q_2 \left(\frac{d\theta}{dq}\right)_2\right\}$$
$$+ \left(\frac{\partial\psi}{\partial\theta}\right)_2 \left\{\left[1-\frac{q_1}{q_2}\cos(\theta_1-\theta_2)\right]\frac{1-(\gamma+1)/(\gamma-1)}{1-q_2^2} + q_1\sin(\theta_1-\theta_2)\left(\frac{d\theta}{dq}\right)_2\right\} = 0, \quad (5.3)$$

which is a relation of the form $F[\partial\psi/\partial q,\ \partial\psi/\partial\theta,\ q_1,\ \theta_1,\ q_2,\ \theta_2,\ dq/d\theta] = 0$ homogeneous in ψ [here it is written at the point (q_2, θ_2)].

These three conditions are sufficient to construct a unique shock curve in the hodograph.

Reference is made here to the original papers by Nocilla (1957, 1958) and to the very comprehensive book by Ferrari & Tricomi (1968), where these papers are discussed. Nocilla shows that the shock curves $S_1 + S_2$ are tangential to the limiting lines at the point where they meet (double point). We recall that, in the physical plane, this point corresponds to the first point on the envelope of a family of characteristics. This is the point where the shock curve starts in this plane. It has infinitesimal strength there (compression Mach wave) since it is tangential to the characteristic through this point.

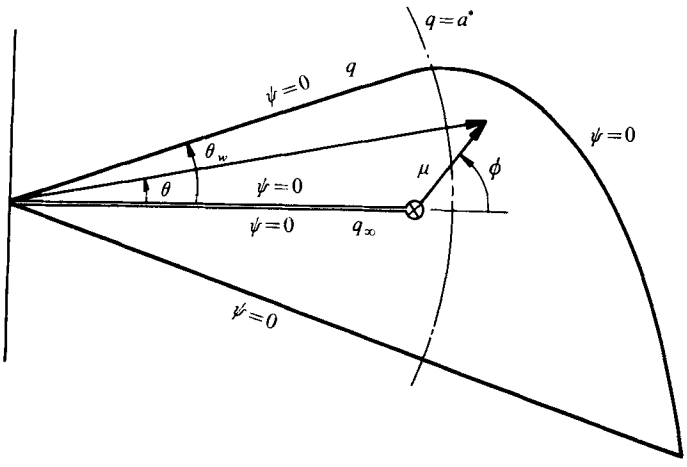

FIGURE 7. Polar co-ordinates at the singular point.

We should note here that in the particular case of the wedge we can construct the shock curve starting either from the double point or from the foot of the shock (D_1, D_2) because we know these points *a priori*, once $\psi(q, \theta)$ is known. More details on this will be given later. We shall now be more specific about the numerical method used to solve for $\psi(q, \theta)$.

6. Numerical solution

As mentioned at the beginning of the present work, we shall use techniques identical to those of Gilinskii *et al.* (1964), but specialized to transonic flows. References dealing with the mathematical basis for the method are to be found in that paper. The method seems to be of great interest when dealing with elliptic or mixed types of equations, because the problem is formulated in terms of an initial-value problem and the last boundary condition is met by iterating successively on one of the initial conditions. The scheme, in comparison with a network difference scheme, is very economical in computer time and the storage required is not large. Needless to say, in working with a linear equation (hodograph equation) the iteration is no longer needed and an elementary linear superposition is all that is required to meet all the boundary conditions. Reference is also given here to a paper by Holt & Ndefo (1970), where the method was used with great success.

Before we set the numerical algorithm, we transform the complex hodograph domain into a rectangular domain.

6.1. *Mapping of the domain onto a rectangle*

First we select a new system of polar co-ordinates (μ, ϕ) with origin at the singular point q_∞ (figure 7). The corresponding formulae are

$$\left.\begin{aligned} \mu &= (q_\infty^2 + q^2 - 2q_\infty q\cos\theta)^{\frac{1}{2}}, \\ \phi &= \tan^{-1}\left(\frac{q\sin\theta}{q\cos\theta - q_\infty}\right) + k\pi. \end{aligned}\right\} \tag{6.1}$$

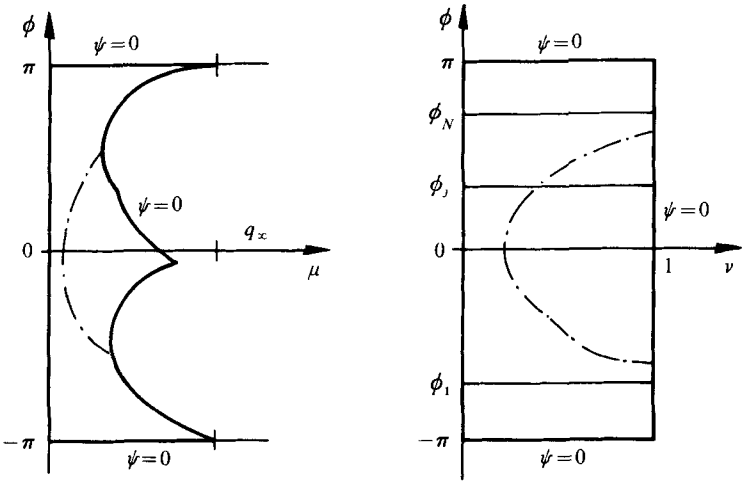

FIGURE 8. Mapping of the hodograph domain onto a rectangle.

Now we define Cartesian co-ordinates by

$$\nu = \mu/\bar{\mu}(\phi), \quad \phi = \phi, \tag{6.2}$$

where $\bar{\mu}(\phi)$ is the analytic approximation to the exact equation of the boundary. See figure 8.

For these new variables the partial differential equation (3.1) assumes the form

$$\bar{A}(\nu,\phi)\frac{\partial^2\psi}{\partial\nu^2} + 2\bar{B}(\nu,\phi)\frac{\partial^2\psi}{\partial\nu\,\partial\phi} + \bar{C}(\nu,\phi)\frac{\partial^2\psi}{\partial\phi^2} + \bar{D}(\nu,\phi)\frac{\partial\psi}{\partial\nu} + \bar{E}(\nu,\phi)\frac{\partial\psi}{\partial\phi} = 0. \tag{6.3}$$

6.2. *Telenin's method*

The solution to (6.3) is written as

$$\psi(\nu,\phi) = \sum_{i=1}^{N} \sin\frac{i(\pi-\phi)}{2}\psi_i(\nu) \tag{6.4}$$

in terms of the trigonometric interpolation polynomials of degree N,

$$\sin[\tfrac{1}{2}i(\pi-\phi)] \quad (i = 1,\ldots,N).$$

Note that by this choice we have already satisfied two boundary conditions (at $\phi = \pm\pi, \psi = 0$).

The $\psi_i(\nu)$ are a linear combination

$$\psi_i(\nu) = \sum_{j=1}^{N} c_{ij}\Psi_j(\nu)$$

of the $\Psi_j(\nu) = \psi(\nu,\phi_j)$ (by definition), where ϕ_j $(j = 1, N)$ is the value of ϕ on the jth ray (see figure 8). The position of the rays is determined by stability considerations. The rays are placed at the zeros of the trigonometric polynomial of degree $N+1$: $\sin(N+1)[\frac{1}{2}(\pi-\phi)]$. A further factor in choosing trigonometric polynomials rather than Lagrange polynomials is that the rays are equally spaced from $\phi = -\pi$ to $\phi = \pi$.

We choose the $\Psi_j(\nu)$ as our unknowns. Hence the partial derivatives can be written on the ray $\phi = \phi_j$ as

$$\left(\frac{\partial \psi}{\partial \nu}\right)_{\phi=\phi_j} = \frac{d\Psi_j}{d\nu},$$

$$\left(\frac{\partial \psi}{\partial \phi}\right)_{\phi=\phi_j} = \sum_{i=1}^{N} -\frac{i}{2}\cos\frac{i(\pi-\phi_j)}{2}\left(\sum_{j=1}^{N} c_{ij}\Psi_j\right),$$

$$\left(\frac{\partial^2 \psi}{\partial \nu^2}\right)_{\phi=\phi_j} = \frac{d^2\Psi_j}{d\nu^2},$$

$$\left(\frac{\partial^2 \psi}{\partial \nu \partial \phi}\right)_{\phi=\phi_j} = \sum_{i=1}^{N} -\frac{i}{2}\cos\frac{i(\pi-\phi_j)}{2}\left(\sum_{j=1}^{N} c_{ij}\frac{d\Psi_j}{d\nu}\right),$$

$$\left(\frac{\partial^2 \psi}{\partial \phi^2}\right)_{\phi=\phi_j} = \sum_{i=1}^{N} -\left(\frac{i}{2}\right)^2\sin\frac{i(\pi-\phi_j)}{2}\left(\sum_{j=1}^{N} c_{ij}\Psi_j\right).$$

On each ray $\phi = \phi_j$ we are left with a second-order ordinary differential equation of the form

$$\frac{d^2\Psi_j}{d\nu^2} = -\frac{1}{\bar{A}(\nu,\phi_j)}\left(\sum_{k=1}^{N}\alpha_{kj}\frac{d\Psi_k}{d\nu} + \beta_{kj}\Psi_k\right), \tag{6.5}$$

$$\alpha_{kj} = \alpha_{kj}(\nu,\phi_j), \quad \beta_{kj} = \beta_{kj}(\nu,\phi_j).$$

Equation (6.5) is solved as an initial-value problem, starting from the boundary $\nu = 1$ and iterating towards $\nu = 0$, with

$$\Psi_j(\nu = 1) = 0, \quad d\Psi_j(\nu = 1)/d\nu = \delta_{jr}, \tag{6.6), (6.7}$$

where $r = 1, \ldots, N$ corresponds to a problem where all the normal derivatives are zero except that at $\phi = \phi_j$.

Since the coefficients become infinite at $\nu = 0$ (a singular point of the solution) we integrate only up to a small circle surrounding A_∞, corresponding to the value $\nu = \nu_0$.

A linear combination of the N problems is chosen which satisfies two conditions. The first condition simply ensures that we have a closed body, i.e.

$$\oint_{\psi=0} dy = 0.$$

This implies a linear relation between the normal derivatives:

$$\sum_i a_i \frac{d\Psi_i}{d\nu}(\nu = 1) = 0. \tag{6.8}$$

The second condition is peculiar to the present problem. Since the foot of the shock is located at D, where the body slope is discontinuous, the flow direction at the body on the upstream side of the shock surface cannot be specified. This is responsible for the non-unique situation, as a result of which the selection of the physically meaningful solution must be realized by means of some criterion. Another case of non-uniqueness is found, for example, in the deflexion of a supersonic flow by a simple wedge across a shock wave, where two such oblique waves can be found. The criterion that the shock generated should be the weakest possible is reasonable and is equivalent, in practice, to selecting the set of normal derivatives which maximizes the value of q_{D_2}:

$$q_{D_2}\left(\frac{d\Psi_i}{d\nu}(\nu = 1)\right) = q_{D_2 \max}. \tag{6.9}$$

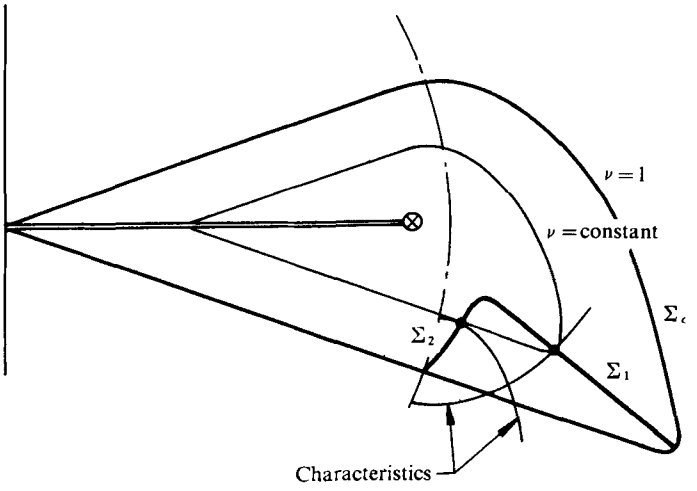

FIGURE 9. Singular lines.

6.3. *Singular lines of the coefficients*

Since (3.1) is of mixed type, the characteristics are real in the hyperbolic subdomain and, in general, one of the co-ordinate curves, ν = constant, say, will be tangential to a characteristic. The curve joining such points of contact is a singular line since it is easily proved that the coefficient of $\partial^2\psi/\partial\nu^2$ vanishes there. It is clear that this will happen in the case of the wedge. There will be two singular lines Σ_1 and Σ_2 because, in particular, the curve $\nu = 1$ has two such points of contact (figure 4). But the assumption of analyticity allows us to cross these lines by analytic continuation.

It should be noted, however, that these lines have no physical significance and are a consequence of the system of co-ordinates chosen. In our particular problem, the curve $\nu = 1$ is also a streamline, therefore the singular lines and the limit lines pass through the same points. The characteristic which is the boundary of the supersonic domain is also a singular line Σ_c (figure 9).

6.4. *Numerical integration*

The system of N simultaneous second-order ordinary differential equations (6.5) together with initial conditions (6.6) and (6.7) is transformed into a system of $2N$ simultaneous first-order ordinary differential equations by setting

$$\Psi_{j+N} = d\Psi_j/d\nu.$$

Hence we obtain the following system S^r:

$$d\Psi_j/d\nu = \Psi_{j+N}, \quad j = 1, \ldots, N,$$

$$\frac{d\Psi_{j+N}}{d\nu} = -\frac{1}{A(\nu, \phi_j)} \sum_{k=1}^{N} (\alpha_{kj}\Psi_{k+N} + \beta_{kj}\Psi_k), \quad j = 1, \ldots, N,$$

$$\Psi_j(1) = 0, \quad j = 1, \ldots, N,$$

$$\Psi_{j+N}(1) = \delta_{jr}, \quad j = 1, \ldots, r, \ldots, N.$$

This is solved using a fifth-order Runge–Kutta scheme with automatic error and step-size controls on a CDC 6400 computer.

7. Transformation to the physical plane: results

Once a solution has been obtained for $\psi(\nu, \phi)$, i.e. for $\psi(q, \theta)$, it is possible to locate the points D_1 and D_2 (figure 2) and to obtain the pressure distribution on the aerofoil and hence the drag.

7.1. *Foot of the attached shock*

The first side of the wedge is represented by the segment BC in the physical as well as the hodograph plane (figures 1 and 2). The rear side is represented by DE in the physical plane and D_1E in the hodograph.

Certainly we must have

$$\int_{BCDE} dy = 0 \quad \text{in both planes,}$$

in particular $$\int_{\substack{BC \\ \psi=0}} dy + \int_{CD_1} dy + \int_{D_2E} dy = 0 \quad \text{in the hodograph.}$$

But $$\int_{CD_1} dy = 0$$

since CD_1 is an arc of a characteristic where $J = \partial(x, y)/\partial(q, \theta) = 0$. Hence it must be true that

$$\int_{BC} dy = \int_{ED_2} dy.$$

Along BC and ED_2, θ = constant and only q varies, furthermore $\psi = 0$, so that $\partial\psi/\partial q = 0$ on both segments. Equation (3.4) yields

$$dy = \frac{\partial y}{\partial q} dq = -\frac{\sin\theta}{\rho q^2}\left(1 - \frac{q^2}{a^2}\right)\frac{\partial \psi}{\partial \theta} dq$$

$$= -\frac{\sin\theta}{q^2}\frac{1 - [(\gamma+1)/(\gamma-1)]\,q^2}{(1-q^2)^{\gamma/(\gamma-1)}}\frac{\partial \psi}{\partial \theta} dq. \tag{7.1}$$

Of course, as q approaches zero, dy is well behaved because $\partial\psi/\partial\theta$ vanishes very rapidly there. The limit is obtained by matching locally the compressible to the incompressible solution. It is easily shown that the incompressible potential at a concave corner yields a derivative $\partial\psi_i/\partial\theta \sim Kq^{\pi/\theta_w}$, θ_w being the half-angle of the wedge. The value of the constant K is found by equating $\partial\psi_i/\partial\theta$ and $\partial\psi/\partial\theta$ at a point where, say,

$$q_i = 0{\cdot}1[(\gamma-1)/(\gamma+1)]^{\frac{1}{2}}.$$

At this point the value of y is

$$y_i = y = K\frac{\theta_w \sin\theta_w}{\pi - \theta_w} q_i^{(\pi-\theta_w)/\theta_w}.$$

Note that the values for K are going to be different at the leading and trailing edges of the wedge. Performing the integration, we obtain at the same time the numerical values of the half-thickness $\frac{1}{2}t$:

$$\tfrac{1}{2}t = (y_i)_{\theta_w} - \sin\theta_w \int_{q_i}^{[(\gamma-1)/(\gamma+1)]^{\frac{1}{2}}} \frac{1 - [(\gamma+1)/(\gamma-1)]\,q^2}{q^2(1-q^2)^{\gamma/(\gamma-1)}}\left(\frac{\partial\psi}{\partial\theta}\right)_{\theta_w} dq$$

$$= (y_i)_{-\theta_w} + \sin\theta_w \int_{q_i}^{q_{D_2}} \frac{1 - [(\gamma+1)/(\gamma-1)]\,q^2}{q^2(1-q^2)^{\gamma/(\gamma-1)}}\left(\frac{\partial\psi}{\partial\theta}\right)_{-\theta_w} dq,$$

which determines the value of q_{D_2}.

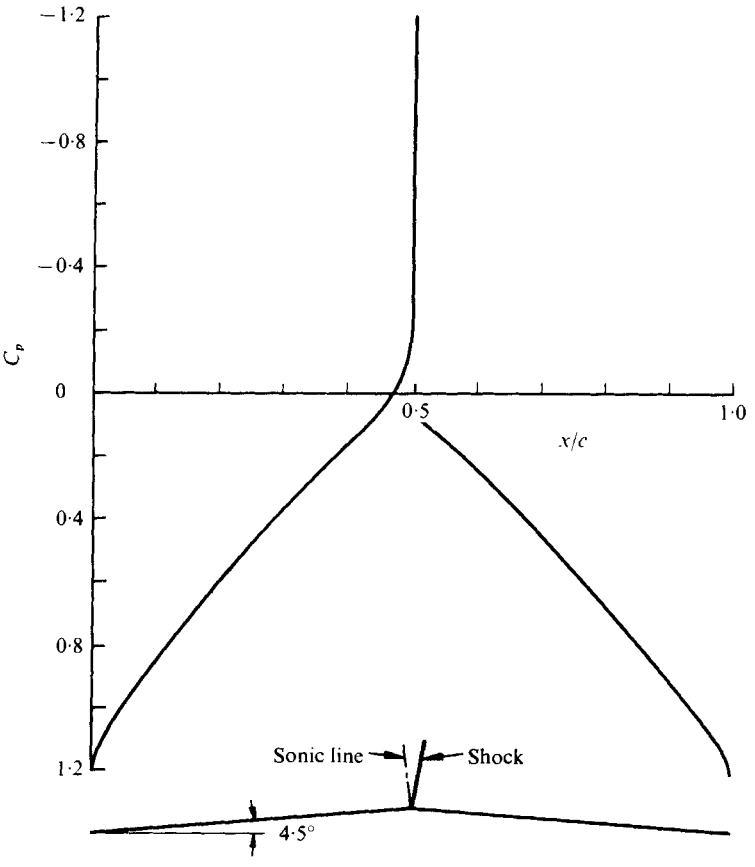

FIGURE 10. Pressure distribution along the double wedge.

7.2. *Pressure distribution on the wedge*

As a by-product of the previous computation we were able to obtain

$$y = y(q). \tag{7.2}$$

This allows us to sketch the distribution of the pressure coefficient C_p on the wedge since the dependence of C_p on the speed is given by

$$\begin{aligned} C_p &= \frac{p-p_\infty}{\frac{1}{2}\rho_\infty \bar{q}_\infty^2} = \frac{\gamma-1}{\gamma}\frac{[(1-q^2)^{\gamma/(\gamma-1)} - (1-q_\infty^2)^{\gamma/(\gamma-1)}]}{q_\infty^2\,(1-q_\infty^2)^{1/(\gamma-1)}} \\ &= C_p(q). \end{aligned} \tag{7.3}$$

Equations (7.2) and (7.3) yield a parametric representation of C_p. (See figure 10.) The discontinuity in C_p at $x/c = 0{\cdot}5$ corresponds to the recompression through the shock at D.

7.3. *Drag*

The drag on the wedge is found by integrating C_p along the aerofoil, which is equivalent to

$$\mathscr{D} = 2\int_{BCDE}(p_s - p)\,dy$$
$$= 2\int_{BC}(p_s - p)\,dy + 2\int_{CD_1}(p_s - p)\,dy + 2\int_{D_2E}(p_s - p)\,dy.$$

Again the middle integral vanishes because CD_1 is an arc of a characteristic where $dy = 0$, so that the total drag is the algebraic sum of the drag on the front part and the drag on the rear part of the wedge. The element dy has the same expression as in (7.1) and is well behaved in the limit as q approaches zero. Also $p_s - p$ vanishes there since p_s is the stagnation pressure.

We use the matching of § 7.1 to compute the contribution to the drag of the part of the aerofoil near the two stagnation points. We obtain

$$\frac{\mathscr{D}}{\frac{1}{2}\rho_\infty \bar{q}_{\max}^2} = -2\sin\theta_w\left\{\int_0^{q_i}\left(\frac{\partial\psi}{\partial\theta}\right)_{\theta_w} dq + \int_0^{q_i}\left(\frac{\partial\psi}{\partial\theta}\right)_{-\theta_w} dq\right\} - 2\frac{\gamma-1}{\gamma}\sin\theta_w$$
$$\times\left\{\int_{q_i}^{[(\gamma-1)/(\gamma+1)]^{\frac{1}{2}}} \frac{[1-(1-q^2)^{\gamma/(\gamma-1)}]\{1-[(\gamma+1)/(\gamma-1)]\,q^2\}}{q^2(1-q^2)^{\gamma/(\gamma-1)}}\left(\frac{\partial\psi}{\partial\theta}\right)_{\theta_w} dq\right.$$
$$\left.+\int_{q_i}^{q_{D_2}} \frac{[1-(1-q^2)^{\gamma/(\gamma-1)}]\{1-[(\gamma+1)/(\gamma-1)]\,q^2\}}{q^2(1-q^2)^{\gamma/(\gamma-1)}}\left(\frac{\partial\psi}{\partial\theta}\right)_{-\theta_w} dq\right\}.$$

The first and the third integrals correspond to the fore drag (they are positive) while the second and last integrals correspond to the drag on the rear part of the wedge (they are negative).

7.4. *Results*

The method is applied to a 4·5° half-angle wedge at a Mach number $M_\infty = 0{\cdot}89$. These figures have been chosen so that the recompression shock will not be too strong for the flow downstream of it to be treated by transonic potential theory.

There is no previous theory with which to compare the results. Cole (1951) used small perturbation theory to solve for the transonic flow past a simple wedge.

Comparison with experiments on a double wedge such as those by Bryson (1952) is not possible since the influence of viscosity on the potential flow field is to change completely the flow pattern on the rear side of the wedge. Viscosity creates a small separation bubble near the convex corner which causes the foot of the shock to move downstream of the shoulder. As a result of this boundary-layer interaction, the supersonic region is, in that case, partly bounded by the rear part of the wedge, which creates a region of very low pressure. This factor is responsible for a large experimental drag.

It should be noted at this point that viscosity will play a less important role for a smooth aerofoil and therefore in this case the present theory would be suitable for predicting the point where the shock actually meets the surface normally, downstream of the point of maximum thickness (figure 1).

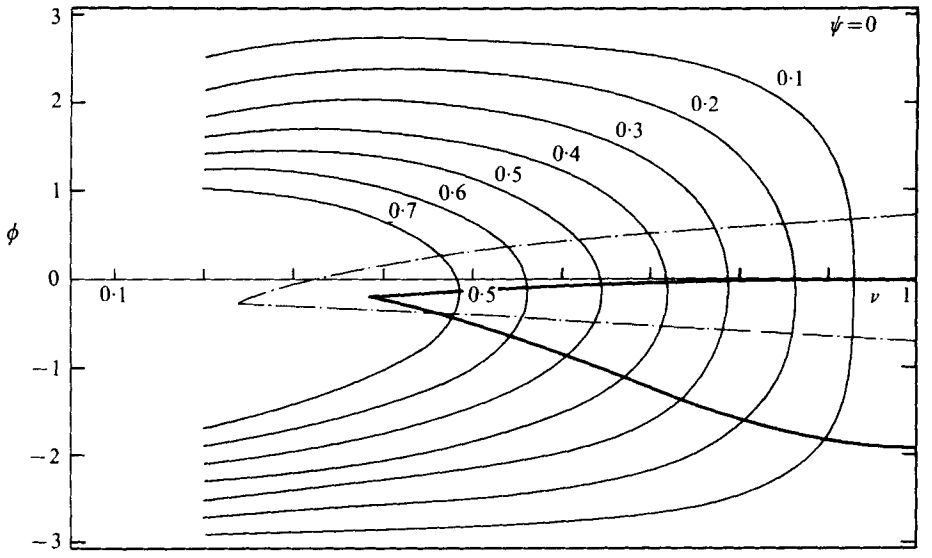

FIGURE 11. Hodograph plane in (ν, ϕ) co-ordinates. ——, streamlines; — · —, sonic lines; ▬, shock wave.

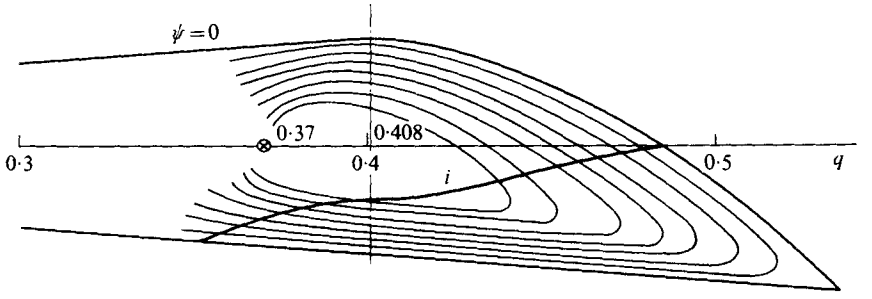

FIGURE 12. Hodograph plane in (q, θ) co-ordinates. ——, streamlines; ▬, shock wave.

The inviscid model we have been using here has enabled us to predict the pressure distribution along the double wedge (figure 10), to construct the pertinent hodograph plane (figures 11 and 12) and to obtain a visualization of the sonic line and the shock wave in the physical plane (figure 13), which confirms what Nocilla (1957, 1958) had foreseen.

The shock curve appears in the middle of the supersonic region, at a point where the Mach number is $M_i = 1{\cdot}05$. The shock is tangential there to the compression Mach wave. It is worth noting that the part of the shock embedded in the supersonic domain is very close to the sonic line which is behind it. This may explain why it is difficult to detect this flow pattern experimentally and the shock is often shown as being coincident with the sonic line.

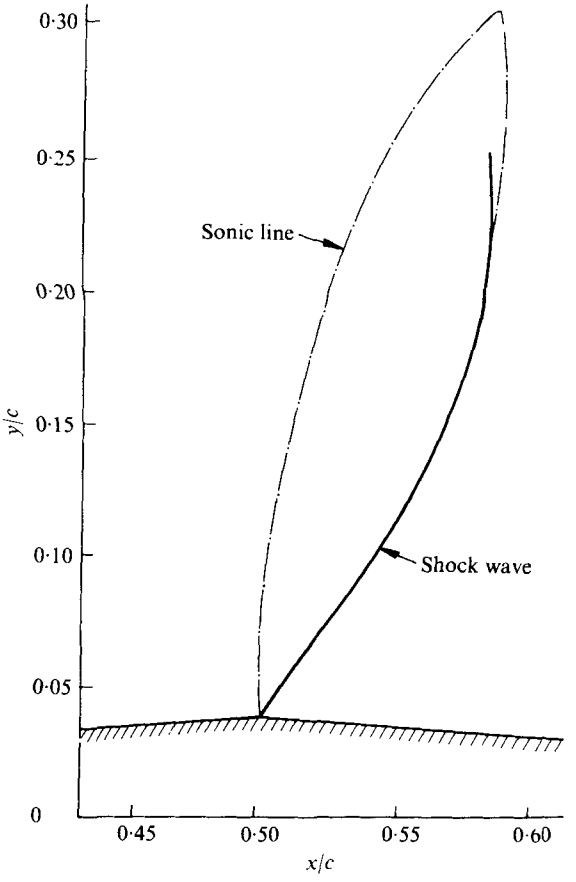

FIGURE 13. Sonic line and shock wave.

8. Conclusion

A solution to the transonic flow past a symmetrical double wedge is constructed in the hodograph plane using Telenin's method. In the case of the flow past a double wedge we know *a priori* the boundary of the domain in the physical as well as in the hodograph plane.

Comparison with experiments is impossible because of the boundary-layer separation. The mathematical model represents the flow past the double wedge in the limit where the Reynolds number approaches infinity.

The solution exhibits the sonic line and the shock curve pertinent to the formulation, and a description of the flow pattern is given in the neighbourhood of the point where the sonic line meets the shock.

This work was submitted in partial fulfilment of the requirements for the degree of Doctor of Philosophy at the University of California, Berkeley. It was supported in part by the Air Force Office of Scientific Research under a Grant supervized by M. Holt.

REFERENCES

BRYSON, A. E. 1952 An experimental investigation of transonic flow past two-dimensional wedge and circular-arc sections using a Mach–Zehnder interferometer. *N.A.C.A. Rep.* no. 1094.

COLE, D. 1951 Drag of a finite wedge at high subsonic speeds. *J. Math. Phys.* **30**, 79–93.

FERRARI, C. & TRICOMI, F. 1968 *Transonic Aerodynamics.* Academic Press.

GERMAIN, P. 1962 Problèmes mathématiques posés par l'application de la méthode de l'hodographe à l'étude des écoulements transsoniques. *Symp. Transsonicum, IUTAM Symp. Aachen*, vol. 2. *Sitzung*, p. 24.

GILINSKII, S. M., TELENIN, G. F. & TINYAKOV, G. P. 1964 A method for computing supersonic flow around blunt bodies, accompanied by a detached shock wave. *Izv. Akad. Nauk SSSR Mekh. i Math.* **4**, 9–28. (See also *N.A.S.A. Trans.* TT F-297.)

HOLT, M. & NDEFO, D. E. 1970 A numerical method for calculating steady unsymmetrical supersonic flows past cones. *J. Comp. Phys.* **5**.

LIGHTHILL, M. J. 1953 The hodograph transformation. In *Modern Developments in Fluid Dynamics – High Speed Flow* (ed. L. Howarth), vol. 1, chap. 7, pp. 222–266. Oxford University Press.

NOCILLA, S. 1957 Flussi transonici attorno a profili alari simmetrici con onda d'urto attaccata ($M_\infty < 1$). *Atti. Accad. Sci. Torino, Classe Sci. Fis. Mat. Nat.* **92**, 282–307.

NOCILLA, S. 1958 Flussi transonici attorno a profili alari simmetrici con onda d'urto attaccata ($M_\infty < 1$). II. *Atti. Accad. Sci. Torino, Classe Sci. Fis. Mat. Nat.* **93**, 124–148.